Macroscopic Quantum Interference in Superconductors

R. C. JAKLEVIC, J. LAMBE, J. E. MERCEREAU, AND A. H. SILVER
Scientific Laboratory, Ford Motor Company, Dearborn, Michigan
(Received 12 July 1965)

The Josephson effect allows supercurrents to flow through thin tunnel barriers separating two superconductors. The dc critical current depends directly on the quantum phase difference of the superconducting wave function on the two sides of the barrier. This paper is an experimental study of interference phenomena in multiply connected superconductors utilizing Josephson tunneling. The results are a striking confirmation of the extensive phase coherence of the superconducting state. London's theory is used in conjunction with Josephson's prediction to explain the observations. Modulation of the maximum supercurrent flow through junction-pair devices was measured in an applied magnetic field and showed periodicities resulting from quantum wave interference. These interference "fringes" were found to occur even when the magnetic flux is confined to a region not accessible to the superconductor. Another experiment allows the measurement of an interference directly attributable to phase modulation by the superconducting electron-drift velocity. These results offer a direct verification of long-range quantum behavior in the superconducting state and further demonstrate the validity and usefulness of Josephson tunneling methods.

INTRODUCTION

FOLLOWING the early suggestion of London,[1] the superconducting state has come to be regarded as one of long-range phase coherence of the superconducting electrons. In the light of all present theories, this may be viewed as a condensation of the paired electrons into a single quantum state in which all of the pairs have identical momentum, $\mathbf{p}=(m^*\mathbf{v}+e^*\mathbf{A})$, where m^* and e^* are twice their free-electron values. This high degree of correlation of the bound electron pairs in the superconducting ground state gives rise to interesting quantum behavior on a macroscopically large scale. It is possible to describe the superconducting state by an effective wave function Ψ for the electrons in which Ψ^2 is equal to the density N of superconducting electrons and γ represents the phase.[2] The quantum-mechanical expression for the current density can be used to write the difference in phase of Ψ between two points in the superconductor;

$$\gamma_2-\gamma_1=-\frac{2e}{\hbar}\int_1^2(\mu_0\lambda^2\mathbf{j}+\mathbf{A})\cdot d\mathbf{l}, \tag{1}$$

where $\mathbf{j}$ is the supercurrent density and $\lambda^2=m(\mu_0Ne^2)^{-1}$ is the London penetration depth and $\mathbf{A}$ the vector potential. If the integration is carried out around a closed loop, the single valuedness of Ψ requires that $\Delta\gamma=2\pi n$ with n and integer. From this it is easy to see that the *fluxoid*, defined by London[3] to be

$$\Phi=\oint(\mu_0\lambda^2\mathbf{j}+\mathbf{A})\cdot d\mathbf{l} \tag{2}$$

should be restricted to values $n(h/2e)$. The London equation for superconductivity assumes $n=0$ in a singly connected material, or $\nabla\times\mu_0\lambda^2\mathbf{j}=-\mathbf{B}$. More recent developments, such as that by Abrikosov,[4] also allow $n=1$, under certain conditions. For a thick superconducting ring it is possible to do the indicated integration around the hole entirely in a current-free region where the field does not penetrate. The fact that $\oint\mathbf{A}\cdot d\mathbf{l}$ is the flux enclosed by the ring predicts that this trapped flux will be quantized in multiples of $h/2e$, by now a well-established experimental fact.[5]

Another more recent development has been the prediction by Josephson regarding direct tunneling of electrons from one superconductor to another through a very thin insulating region (10–20 Å).[6] His calculation indicated that, in addition to the tunneling of single electrons with the accompanying voltage drop across the junction, there should also be a coherent tunneling of the condensed pairs from one superconductor to the other. The oxide layer behaves in a manner analogous to superconductors and the junction is expected to allow the passage of a dc current without developing a voltage across the insulator (Fig. 1). Another closely related effect is the prediction that an ac supercurrent of frequency $2eV/h$ should appear whenever a voltage V is applied across the junction. This unusual behavior is a result of a coherent coupling of the two superconducting wave functions by tunneling causing superconducting transfer across the insulator region.

In particular, for the dc case, Josephson's prediction for the supercurrent density is

$$j=j_0\sin\left(\gamma_2-\gamma_1-\frac{2e}{\hbar}\int_1^2\mathbf{A}\cdot d\mathbf{l}\right), \tag{3}$$

where γ_1 and γ_2 are the phases of the superconducting wave functions on the opposite sides of the barrier. For identical superconductors on both sides, the low-

[1] F. London, Proc. Roy. Soc. (London) **A152**, 24 (1935).
[2] L. P. Gor'kov, Zh. Eksperim. i Teor. Fiz. **36**, 1918 (1959) [English transl.: Soviet Phys.—JETP **9**, 1364 (1959)].
[3] F. London, *Superfluids* (John Wiley & Sons, Inc., New York, 1950), Vol. 1.
[4] A. A. Abrikosov, Zh. Eksperim. i Teor. Fiz. **32**, 1442 (1957) [English transl.: Soviet Phys.—JETP **5**, 1174 (1957)].
[5] B. S. Deaver and W. M. Fairbank, Phys. Rev. Letters **7**, 43 (1961); R. Doll and M. Näbauer, *ibid.* **7**, 51 (1961).
[6] B. D. Josephson, Phys. Letters **1**, 251 (1962); Rev. Mod. Phys. **36**, 216 (1964).

temperature value for j_0 is $\pi\Delta(2\sigma R_n)^{-1}$ with Δ the half-value of the two-particle superconducting energy gap in volts, R_n the resistance of the tunneling layer when both metals are normal, and σ the area of the junction. The term containing the line integral of the vector potential between the two sides must appear in order that the expression be invariant under a gauge transformation. To include the ac effects, a term $\hbar^{-1}\int V dt$ is needed in the phase difference corresponding to a rotation of the relative phase at a frequency $2eV/h$ giving rise to the ac current. Since this paper will be confirmed to a discussion of dc phenomena, this part will be ignored. The reality of the dc Josephson effect was first established by Anderson and Rowell[7,8] who also found that the Josephson current through a single junction is a periodic function of the flux enclosed in the junction. Phenomena directly attributable to the ac current-flow prediction have been observed by Shapiro and others.[9]

We have previously briefly reported experiments in which multiply connected superconductors containing two Josephson junctions were studied.[10] The critical supercurrent of these devices is a periodic function of the flux enclosed by the circuit, including the situation in which the field has no access to any part of the circuit. In addition, interference effects attributable to supercurrent flow in one of the films were observed and measured in the absence of any changes in the enclosed flux. After a brief exposition of theoretical expectations, the experiments are described in some detail.

THEORETICAL CONSIDERATIONS

Ideal Single and Double Junctions in a Uniform Applied Magnetic Field

Since it is not the actual point value of the phase which determines the Josephson current, but rather the relative values across the oxide, it is necessary to take into account the modifications due to a magnetic field

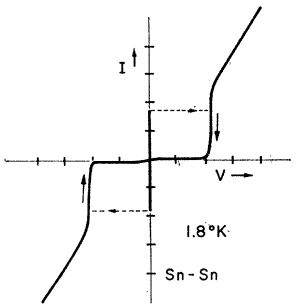

FIG. 1. Reproduction of an oscilloscope trace of a single Sn-SnO_x-Sn junction showing the single-particle (Giaever) tunneling characteristic ($V\neq 0$) and the dc Josephson supercurrent at $V=0$. Current and voltage scales are 0.5 mA/div and 1 mV/div, respectively. The arrows indicate the switching path along the circuit load line taken when the applied current exceeds I_{max}.

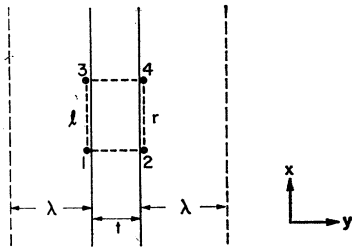

FIG. 2. Schematic cross section of a Josephson junction (not to scale) with magnetic field in z direction. Dotted lines indicate path of integration taken for relative phase determination.

present in the barrier region. It is this modification, first demonstrated by Rowell,[8] which is probably the main reason the effect had not been observed sooner; for junctions of ordinary dimensions the earth's field is sufficient to quench these supercurrents. The behavior of a Josephson junction of width w with an applied field $\mathbf{B}$ threading through the junction can be computed by summing the current density [Eq. (3)] over the entire area of the junction. The field is parallel to the oxide layer and penetrates a distance λ into the identical superconductors (Fig. 2). If the center of the junction is at $x=0$, the phase changes δ across the barrier at the points 0 and x are

$$\delta(0)=\gamma_2(0)-\gamma_1(0),$$
$$\delta(x)=\gamma_4(x)-\gamma_3(x),$$

while the phase differences within a single superconductor are given by

$$\gamma_3(x)-\gamma_1(0)=\frac{1}{\hbar}\int_0^x \mathbf{p}\cdot d\mathbf{l} \quad \text{(left side)},$$
$$\gamma_2(0)-\gamma_4(x)=\frac{1}{\hbar}\int_x^0 \mathbf{p}\cdot d\mathbf{l} \quad \text{(right side)}. \tag{4}$$

At the surface of the superconductors where these integrals will be evaluated the currents are parallel to the surface and their contribution to the phase difference is not negligible. Choosing a gauge such that the component of $\mathbf{A}$ perpendicular to the junction at $x=0$ is zero, it then follows that the argument of Eq. (3) reduces to

$$\delta(0)+\frac{2e}{\hbar}\left\{\Phi(x)+2\int_0^x \mu_0\lambda^2 j_s dx\right\}, \tag{5}$$

where $\Phi(x)$ is the flux enclosed in the barrier out to position x. In the presence of a field $\mathbf{B}$ the surface current j_s is $B/\mu_0\lambda$ or

$$j(x)=j_0\sin\{\delta(0)+(2e/\hbar)Bx(t+2\lambda)\}, \tag{6}$$

where t is the oxide thickness. The total current is obtained by integrating from $-w/2$ to $w/2$ giving

$$I=I_0\frac{\sin(\pi\Phi_j/\Phi_0)}{\pi\Phi_j/\Phi_0}\sin\delta(0), \tag{7}$$

where $\Phi_j=B(2\lambda+t)w$ is the flux enclosed by the effective cross-sectional area of the junction, $\Phi_0=h/2e\approx 2.1$

[7] P. W. Anderson and J. M. Rowell, Phys. Rev. Letters **10**, 230 (1963).
[8] J. M. Rowell, Phys. Rev. Letters **11**, 200 (1963).
[9] S. Shapiro, Phys. Rev. Letters **11**, 80 (1963); R. E. Eck, D. J. Scalapino, and B. N. Taylor, *ibid.* **13**, 15 (1964); D. D. Coon and M. D. Fiske, Phys. Rev. **138**, 744 (1965).
[10] R. C. Jaklevic, John Lambe, A. H. Silver, and J. E. Mercereau, Phys. Rev. Letters **12**, 159 (1964); **12**, 274 (1964); Proceedings of the Ninth International Conference on Low Temperature Physics (to be published).

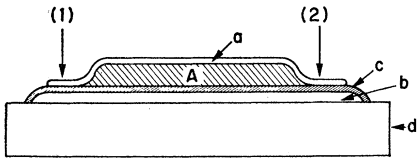

FIG. 3. Schematic of a junction pair (1) and (2) connected by superconductors a and b. The two are separated by the thin oxide layer c and form a loop enclosing the area A. Current flow is measured between a and b.

$\times 10^{-7}$ G cm^2 and $I_0=j_0\sigma$. The phase difference $\delta(0)$ adjusts to the experimental conditions and is zero for no current flow. As the current is increased $\delta(0)$ changes to give maximum positive current flow at $\delta(0)=\pm\pi/2$. The appropriate expected dependence of $I_{\max}$ on the enclosed flux is

$$I_{\max}=I_0\left|\frac{\sin(\pi\Phi_j/\Phi_0)}{\pi\Phi_j/\Phi_0}\right|. \tag{8}$$

Equation (8) represents the diffraction effect for a single Josephson junction in an applied field. $I_{\max}$ is reduced to zero when Φ_j is an integral multiple of $h/2e$.

Another consideration relates to a binding energy per unit area associated with the coupling of the wave functions in the oxide region.[6] Its magnitude is

$$E_{\text{binding}}=\left(\frac{\hbar}{2e}\right)j_0\cos\left(\gamma_2-\gamma_1-\frac{2e}{\hbar}\int_1^2\mathbf{A}\cdot d\mathbf{l}\right), \tag{9}$$

where $(\hbar/2e)j_0\sigma$ is of the order of 1 eV for a typical junction. This energy becomes quite small when the superconductors are separated relatively large distances, roughly more than 50 Å, so the phases are easily uncoupled by thermal fluctuations. However, when this energy becomes larger than kT, thermal fluctuations can no longer decouple the two sides, and the Josephson effect should then be observable. In actual situations, the circuit is connected to room temperature through electrical leads and junctions with theoretical $j_0\sigma$ of 20 μA will be decoupled by thermal effects. This corresponds to normal resistances above about 20 Ω. Junctions with close to the theoretical $j_0\sigma$ were always less than 1 Ω normal resistance and the observed current fell off much faster than $1/R_n$ above 1 Ω. Above 15 Ω the currents were unobservable. The energy of this binding is also seen to vary in a manner just "out of phase" with the supercurrents, and is a maximum when the currents are zero. It is expected that the maximum possible Josephson current will occur together with a minimum in this binding energy.

It has been assumed that the magnetic field extends through the junction cross section without appreciable self-shielding. This is justified providing the width is less then a characteristic length $2\lambda_J$, which is given by[6,11]

$$\lambda_J^{-2}=2(2e/\hbar)\lambda\mu_0 j_0. \tag{10}$$

[11] R. A. Ferrell and R. E. Prange, Phys. Rev. Letters **10**, 479 (1963).

When the junction width is large compared to λ_J, the applied magnetic field is screened from the interior of the junction due to the flow of the Josephson currents themselves. This is closely analogous to the penetration depth λ of an ordinary superconductor. In fact Josephson junctions behave in some ways like a type-II superconductor in that the magnetic field will penetrate a distance $2\lambda_J$ as long as the field is less than a critical field $B_{c_1}=(h/2e)(2\pi\lambda\lambda_J)^{-1}$ and above this, will penetrate the junction in units of Φ_0. For our junctions, λ_J was typically 1 mm and, for all but a very few cases the widths w were less than 0.8 mm. Therefore uniform penetration of the applied magnetic field is assumed to take place across the width of the junctions.

These ideas can be extended to the case of two junctions connected in parallel (Fig. 3). The total current will now be

$$I=I_{10}'\sin\delta_1+I_{20}'\sin\delta_2, \tag{11}$$

where δ_1 and δ_2 are the phase differences across the junctions in the sense of Eq. (7) and the diffraction effects are contained in I_{10}' and I_{20}'. A uniform magnetic field applied perpendicular to the loop will thread through the junctions and area enclosed by the interferometer.

If (1) and (2) are connected by superconducting links, δ_1 and δ_2 are not random but are related by Eq. (4) as long as phase coherence persists;

$$\delta_1=\delta_2-\frac{1}{\hbar}\oint_{\text{s.c.}}\mathbf{p}\cdot d\mathbf{l}. \tag{12}$$

The integral encloses the superconducting loop excluding the junctions. Assuming identical diffraction patterns for the two junctions, the total current flow becomes

$$I=2I_0\frac{\sin(\pi\Phi_j/\Phi_0)}{\pi\Phi_j/\Phi_0}\cos\left(\frac{1}{2\hbar}\oint_{\text{s.c.}}\mathbf{p}\cdot d\mathbf{l}\right)\times\sin\left[\tfrac{1}{2}(\delta_1+\delta_2)\right]. \tag{13}$$

Again, $(\delta_1+\delta_2)$ is free to adjust to the experimental conditions which determine the applied current and gives for the maximum supercurrent flow

$$I_{\max}=2I_0\left|\frac{\sin(\pi\Phi_j/\Phi_0)}{\pi\Phi_j/\Phi_0}\right|\left|\cos\left(\frac{1}{2\hbar}\oint_{\text{s.c.}}\mathbf{p}\cdot d\mathbf{l}\right)\right|. \tag{14}$$

The integral is, explicitly

$$\frac{1}{2\hbar}\oint_{\text{s.c.}}\mathbf{p}\cdot d\mathbf{l}=\frac{m}{\hbar}\oint_{\text{s.c.}}\mathbf{v}\cdot d\mathbf{l}+\frac{e}{\hbar}\Phi_T. \tag{15}$$

where Φ_T is the total flux enclosed by the circuit. The mechanical-momentum term is usually quite small and for now will be neglected. In this case the maximum supercurrent flow through the junction pair ("inter-

ferometer") is

$$I_{\max}=2I_0\left|\frac{\sin(\pi\Phi_j/\Phi_0)}{\pi\Phi_j/\Phi_0}\right|\left|\cos(\pi\Phi_T/\Phi_0)\right|. \quad (16)$$

The total flux Φ_T has as its sources the flux due to external field Φ_a, and also an inductive contribution due to the currents themselves. This inductive flux arises from a current-geometry unbalance during the measurement and from the fact that Eq. (12) requires a circulating screening current to exist even before the external current is applied. This circulating current is analogous to that set up in ordinary superconducting rings which in that case keep the enclosed flux an integral multiple of $h/2e$. In this case it is not possible for the circulating currents to exceed I_0. Therefore, if $LI_0\ll\Phi_0$, where L is the self-inductance of the loop, the self-screening will be very small and it is permissible to set the enclosed flux Φ_T equal to the applied flux Φ_a in Eq. (16).

Now, in addition to the diffraction envelope, there is an additional "interference" effect, with a periodicity in the maximum Josephson current associated with changes of $h/2e$ in the applied flux. This structure will be much more closely spaced in field than the diffraction peaks because of the large difference in the areas. The effective area for the parallel film geometry of this experiment will be $(2\lambda+d)W$, where d is the separation of the films, and W the junction separation. The penetration depth in most cases is much smaller than the film separation so that this periodicity is only slightly dependent on temperature, in contrast to the single junction diffraction pattern, which will reflect the temperature dependence of 2λ very strongly.

If one of the superconductors (say film b of Fig. 3) carries an additional surface current j_D, then the mechanical momentum contribution of this current cannot be neglected. The analytic expression for the maximum supercurrent flow through the junction pair under these circumstances follows from exactly similar reasoning that lead to the flux-dependent interference. Using Eqs. (3), (5), and (14) now with an additional current density (j_D) in the base arm of the interferometer leads to

$$I_{\max}=2I_0\frac{|\sin((e/\hbar)[\Phi_j+\mu_0\lambda^2 j_D w])|}{|(e/\hbar)[\Phi_j+\mu_0\lambda^2 j_D w]|}\times\left|\cos\left(\frac{e}{\hbar}[\Phi_T+\mu_0\lambda^2 j_D W]\right)\right|, \quad (17)$$

where w is the width of the junction in the direction of current flow and W the separation of the junctions on the base film. Again we have an interference phenomenon but this time the periodicity can be associated with changes in the current density of the base film.

Nonideal Behavior of Junction Pairs

The simple form for $I_{\max}$ of Eq. (13) is a result based on the assumptions that the two junctions are identical and is particularly simple when self-screening of flux from the interferometer is a small effect. In practice it is seldom that either of these requirements are met. First, the diffraction pattern of the junction can differ due to differences in width and area causing different diffraction periodicity and unequal maximum current density. Secondly only a few of the junction pairs could be constructed with small enough area to keep the inductance low and thus avoid the self-screening. Especially for those which needed large areas to accommodate a solenoid, the self-inductance was large enough that definite signs of self-screening were present.

To estimate the effect of the first cause of nonideal behavior, it is possible to calculate the maximum possible Josephson current from Eq. (11), assuming $I_{01}'\neq I_{02}'$ and $\Phi_T=\Phi_a$, as a function of applied flux. The sample calculations indicate that when the diffraction amplitudes of the junction are not equal, both the shape and amplitude of the interference pattern is changed. With the reduction in interference modulation, the individual fringes become more nearly sinusoidal, departing from the cusp-like shape predicted by (16). The interference minima are $|I_{20}'-I_{10}'|$ and the maxima are $I_{01}'+I_{02}'$. Whenever one of the junctions, say I_{01}', goes through a zero in its diffraction pattern, the critical current will be I_{02}' with no interference modulation.

The second cause of nonideal behavior is that of the self-screening whenever the self-inductance of the loop becomes large, or when $LI_0\gtrsim\Phi_0$. Under this condition, the internal flux will not be equal to the applied flux except when $\Phi_T=n(h/2e)$ and no external currents are applied. Furthermore, the applied currents will themselves be large enough to introduce a flux. The analysis of all possible situations is very difficult, but it was possible to compute the behavior numerically of some model pairs in which the leads were not connected to the loop at a point of geometrical symmetry and the junction strengths were not identical. We will describe some of the features which we believe represent the kind of behavior to be expected. If $LI_0\lesssim\Phi_0$, the total modulation remains twice the smallest single junction amplitude, but with a distortion of the shape of the interference peaks and a shift of the point at which they reach their maximum. When $LI_0>\Phi_0$, the situation becomes much more complicated. The maximum values of the computed Josephson current become multiple valued, with the number of possibilities increasing with LI_0. This behavior can be seen in actual practice when the I-V characteristics are traced at a frequency of several hundred cycles per second on an oscilloscope (Fig. 4). The circuit selects one of the possible maximum currents in each of the sampling cycles in an apparently random fashion. However, it tends to those values which give largest values of the maximum current. The numerical examples computed indicate that these choices are ones for which, in the initial state before current is applied, the loop tends to small values of the circulating screening current. This is reasonable since these are the states

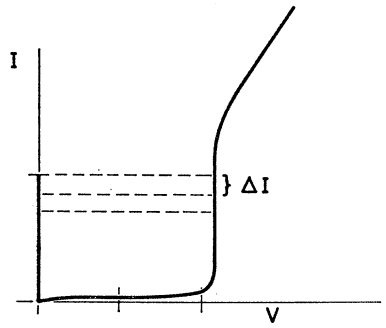

FIG. 4. Representation of experimentally observed multiple-valued maximum Josephson current displayed on an oscilloscope at 350 cps. The current at $V=0$ can attain three possible maximum values before switching along the circuit load line (dashed lines) to the normal tunneling characteristics.

which cost the least energy. A change in applied flux of one quantum unit is necessary to shift the structure in Fig. 4 by ΔI. Since an average of all these possible choices is the actually measured quantity, the over-all effect of increasing LI_0 is a reduction of the amplitude of I_{max} periodicity. This reduction becomes especially severe for the experimental situations where the areas must be made large to accommodate a solenoid.[12] Nevertheless from the examples computed, and from the experiments, the over-all periodicity of the modulation of the maximum measured Josephson current remains equal to a change of $h/2e$ in the *applied* flux through the junction loop.

Superconducting Interferometry

Three types of experiments are reported here utilizing the superconducting interferometer. The first will be a demonstration of the flux-dependent phase shift provided by a uniform magnetic field as explicitly exposed in Eq. (16). The expectation from Eq. (16) is a diffraction modulated interference pattern in the maximum supercurrent flow with interference peaks separated by a flux increment $(h/2e)$.

The second experiment reported here will be the use of the interferometer as a flux meter in the absence of a field. In 1949, Ehrenberg and Siday[13] pointed out that interference patterns observed in an electron microscope should depend on the magnetic flux enclosed by the accessible paths, even when there is no magnetic field available to the electrons. In this experiment, when a single-electron beam is split into two paths and then recombined, interference patterns occur. In the presence of an applied magnetic field, the interference pattern is shifted by an amount proportional to the flux enclosed in the circuit, with a unit of flux h/e necessary to shift the pattern a single period. The result is that flux

$$\Phi=\oint \mathbf{A}\cdot d\mathbf{l}$$

alone can cause such a shift in the absence of any classical forces on the electrons. This was later discussed extensively by Aharonov and Bohm[14] who showed in detailed arguments that this behavior should occur and pointed out that the effect is nonclassical in origin and arises from the single valuedness imposed on the wave function. Their conclusions have opened discussions concerning the physical significance of the vector potential $\mathbf{A}$ as being more than a mathematical convenience. Experiments on this effect have been carried out by a number of experimenters using electron beam techniques, confining the flux either by a ferromagnetic fiber or a closely wound solenoid.[15]

It has been pointed out that an analogous situation occurs for multiply connected superconductors[16] and that macroscopic quantization is another example whereby the behavior of a charged particle depends on flux not directly accessible to the particle. In this connection if the ideas regarding the coherence of the superconducting ring were true, it should be possible to perform the interference experiments previously done with electron beams with the double-junction superconducting "interferometer." In place of the uniform applied field we substitute a long thin solenoid to confine all the flux inside the coil and away from the superconducting circuit. In this case, since the field is confined to the solenoid, there is no flux change in the junctions themselves and the flux will be determined only by the solenoid and not the interferometer geometry. Therefore, diffraction effects of the individual junctions and the slight temperature dependence of the periodicity due to a change of interferometer area will not be present. The effect expected by this technique will be nondiffraction modulated interference produced directly by the static vector potential. The new feature for this particular experiment is that the interfering "particles" are not electrons but pairs. We expect the important term in the relative phase for a shift of exactly one period to be $h/2e$, instead of h/e found for electrons.

The third experiment reported here was designed to observe the quantum phase shifts arising from the electron motion. This type of phase shift was neglected in Eq. (16) as being negligible relative to the flux effect. This third experiment was designed to expose this velocity-dependent phase shift explicitly included in Eq. (17) and

[12] This probably explains the lack of success of some of the early experiments on flux quantization. J. E. Mercereau and L. L. Vant-Hull, Bull. Am. Phys. Soc. **2**, 121 (1961).

[13] W. Ehrenberg and R. E. Siday, Proc. Phys. Soc. (London) **B62**, 8 (1949).

[14] Y. Aharonov and D. Bohm, Phys. Rev. **115**, 485 (1959); **123**, 1511 (1961).

[15] R. G. Chambers, Phys. Rev. Letters **5**, 3 (1960); G. Möllenstedt and W. Bayh, Naturwiss. **49**, 81 (1962); H. Boersch, H. Hamsich, and K. Grohmann, Z. Physik **169**, 263 (1962).

[16] L. Onsager, Phys. Rev. Letters **7**, 56 (1961); L. Onsager, *Proceedings of the International Conference of Theoretical Physics Kyoto and Tokyo, September 1953* (Science Council of Japan, Tokyo 1954), p. 935.

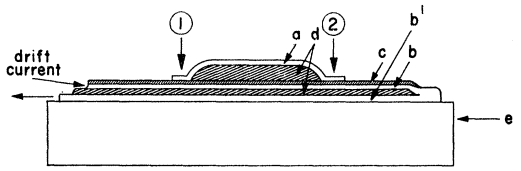

FIG. 5. Schematic of a junction pair (1) and (2) similar to Fig. 3 where the base film strip b carries a drift current which is returned beneath itself by a second base film b' designed to keep the field due to the drift current from the area enclosed by the junction loop. The insulating layers d are of Formvar.

suppress the flux dependence. The arrangement is depicted in Fig. 5 where it can be seen that the base film (b) is turned back under itself in a hairpin geometry which prevents magnetic field associated with a drift current in the base film from extending outside of the base film. This hairpin film is wider than the Josephson junctions. The junctions are connected by the superconducting film (a) forming an interferometer loop in the same manner as the previously described experiments. So, in this arrangement the phase between (1) and (2) will be seen to be affected directly by the drift current in the base film but there will not be any variations in the phase due to a magnetic field arising from the current. From Eq. (17) it can be seen that the period in j_D associated with the separation of the junctions is

$$\Delta j_D = (h/2e)(1/\mu_0\lambda^2 W), \tag{18}$$

while that due to the finite width of the junction will be

$$\Delta j_D = (h/2e)(1/\mu_0\lambda^2 w), \tag{19}$$

with twice this value for the central maximum of the diffraction. The ratio of these is just w/W which involves only the geometry and serves as a convenient check on this result. Since the penetration depth λ is temperature-dependent, the current period Δj_D is also. It remains to relate (18) to the total drift current ΔI_D which is the experimentally varied quantity. Temperature effects are of prime importance through the temperature dependence of the penetration depth. We may take for the temperature dependence of λ the Gorter-Casimir law

$$\lambda^2 = \lambda_0^2[1-(T/T_c)^4]^{-1/2}. \tag{20}$$

The simplest assumption is that the current density is uniform across the thickness of the junction, in which case the period of maximum Josephson current for the interference pattern will be simply proportional to Δj_D. A more realistic model for the current would be that obtained from the Ginzberg-Landau theory which gives, for the surface current density[17]

$$j_D = \frac{I_D}{l\lambda}\frac{1}{\sinh(s/\lambda)}. \tag{21}$$

This, for tin, is the same result obtained from London theory. In this assumption the drift-current periodicity will be

$$\Delta I_D = \frac{l\pi h}{t\mu_0 e W}\left(\frac{s}{\lambda}\right)\sinh\left(\frac{s}{\lambda}\right), \tag{22}$$

where s is the thickness and l the width of the base film. It has been assumed in the foregoing that the actual measuring current used in the determination of I_{max} is not so large as to appreciably affect the supercurrent density.

EXPERIMENTAL TECHNIQUE

The experimental technique for fabrication of the tin-tin oxide-tin tunnel junction differs in some details from previous methods.[18] The base tin layer was deposited in a vacuum of 10^{-6} Torr on cleaned glass or fused silica substrates with standard commercial grade polished surfaces. A large 2 ft^2 copper plate inside the bell jar was cooled to liquid-nitrogen temperature to trap water vapor and other condensable gases. The substrate-mask assembly was mounted in contact with another copper plate cooled to liquid-nitrogen temperature. Thicknesses near 1000 Å were standard for all films. Electron microscope examination of surface replicas of these films showed that considerably smoother surface resulted from the cooling. After deposition of the base film, the substrates were warmed to room temperature in vacuum and removed for further processing. The base film was masked with a plastic film of Formvar[19] to delineate the junction areas and build up the thick areas enclosed by the final junction pair. This plastic film also served to prevent any edge of the base film from being included in a tunnel junction. It was determined that shorts occurred preferentially at these edges, probably due to the breakup at the edges of the base film. After drying the Formvar film for several hours, the oxide was thermally grown on the exposed junction regions by exposure to dry flowing tank oxygen for 1 h at 110°C. The second, top film was then deposited in vacuum at room temperature. Junctions made this way had normal resistance at 4.2°K of 0.05 to 0.5 Ω mm^2. Josephson currents ranged from 0.1 to 1.0 mA at 2°K and junction areas from 0.1 to 0.3 mm^2. The majority of the junctions made by this technique were successful, but more improvement in technique is necessary to insure continuous reliability and reproducibility. If these completed junctions were left at room temperature for a period of more than 1 or 2 days, signs of deterioration became evident. Shorts appeared through the oxide film when the films were superconducting and showed poor electron tunneling characteristics. Attempts to prevent this by applying protective coatings of SiO_x or plastic films over the completed structure did not improve this situation and it is likely that diffusion of tin into the oxide takes place at room temperature.

[17] V. L. Ginzburg, Dokl. Akad. Nauk. SSSR **118**, 464 (1958) [English transl.: Soviet Phys.—Doklady **3**, 102 (1958)].

[18] Ivar Giaever and Karl Megerle, Phys. Rev. **122**, 1101 (1961).

[19] Shawinigan Resins Corporation. The Formvar is dissolved in ethylene chloride or dioxane and applied with a fine brush.

Figure 1 is a reproduction (taken from an oscilloscope face) of an actual I-V plot of one of these junctions. The single particle tunneling curve first studied by Giaever is evident, showing the sharp threshold at $V=2\Delta$ with the current rising to the ohmic part of the characteristic. The normal resistance of the junction is measured from this portion of the trace. At $V=0$ the Josephson supercurrent is seen, which for this junction is 80% of theoretical magnitude. At the start of the tracing cycle, the voltage across the junction remains at $V=0$ until $I_{\max}$ is reached, at which time it switches to the normal curve along the circuit load line and traces out this curve until the voltage again reaches zero at which point it starts over again in the Josephson regime, this time in the negative direction. The most successful junctions exhibited maximum currents greater than one-half the predicted $\frac{1}{2}\pi\Delta R_n^{-1}$ with a few exceeding 90%. When shorts were present, the Giaever-type curve became washed-out and the Josephson current could not be reduced to zero by the application of a magnetic field. For no junction did the maximum supercurrent exceed the predicted value. In the initial testing of a junction, it is necessary to cool it while shielding from the earth's magnetic field. Otherwise flux is apparently trapped in the films or junctions, severely attenuating the Josephson current.

Multiple-junction structures were made following the the above procedure and required more elaborate masking techniques. The masks were made from 3-mil stainless-steel sheet stock spot welded or epoxy-bonded to aluminum frames. The insulation needed to create the area separating the two films was built up with multiple layers of Formvar, from 1 to 20 μ thick. On occasion, collodian films were also used. A typical test sample slide is shown in Fig. 6 which depicts a completed double junction structure together with the electrodes. These electrodes were of fired silver paint (Englehard 32-A) through which the electrical leads were connected to the sample.

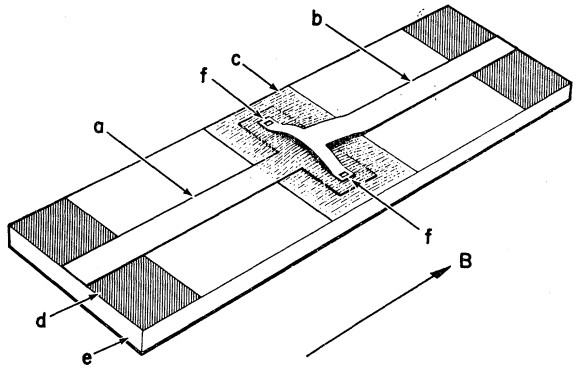

FIG. 6. Schematic of a completed junction pair. A uniform magnetic field is applied parallel to the long dimension of the substrate e. The Formvar insulator c is applied over the base tin film a to mask out the junctions f and separate a from the second tin film b.

Measurements were made with the sample immersed in liquid helium whose temperature could be controlled by a pressure regulated high-speed vacuum pump. A standard Pyrex double Dewar container with 2-liter capacity was used. A vacuum sealed cap was provided for the Dewar through which shielded lead-throughs carried the electrical leads down to the sample. A lead cylinder with a diameter of $2\frac{1}{2}$ in. and 7 in. length was in place around the samples during measurements to screen them from stray magnetic fields. The whole Dewar was surrounded by a double-walled mu-metal cylinder to provide for further shielding. The recording traces of the maximum Josephson current versus the applied magnetic field were obtained conveniently by use of an ac averaging technique. A current source drives the sample at 350 cps with a current amplitude always exceeding the maximum possible Josephson current. The voltage signal is amplified with a high-impedance low-noise preamplifier. This voltage is detected with a full wave (or half-wave) phase sensitive detector. The average dc signal output from this detector is introduced on the Y axis of an X-Y plotter, the X axis being driven by the coil current producing the magnetic field. Because the magnitude of the maximum Josephson current determines the relative time the interferometer voltage remains at $V=0$, changes in the average dc signal are proportional to the maximum Josephson current. This is true for currents greater than about 100 μA. Below this level the simple proportionality is lost and the response is sublinear. However, such detail was not considered of importance for the purposes of the experiments reported here.

The small solenoids were constructed by closely winding a fine insulated copper wire around a beryllium-copper core with the core providing the return path. This was done on a small fixture designed to rotate the core. One type was of 1-mil wire wound on a 3 mil core giving an over-all diameter, including insulation, of 6 mils. A second size was similarly constructed of $\frac{1}{2}$ mil wire around a 1 mil core, with an over-all diameter of 2.2 mils. These were made in batches of four or more and within a given batch were identical in number of turns and length of windings. The calibration was done

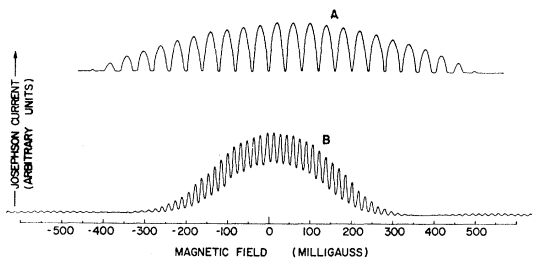

FIG. 7. Experimental trace of $I_{\max}$ versus magnetic field showing interference and diffraction effects. The field periodicity is 39.5 and 16 mG for A and B, respectively. Approximate maximum currents are 1 mA (A) and 0.5 mA (B). The junction separation is $W=3$ mm and junction width $w=0.5$ mm for both cases. The zero offset of A is due to a background magnetic field.

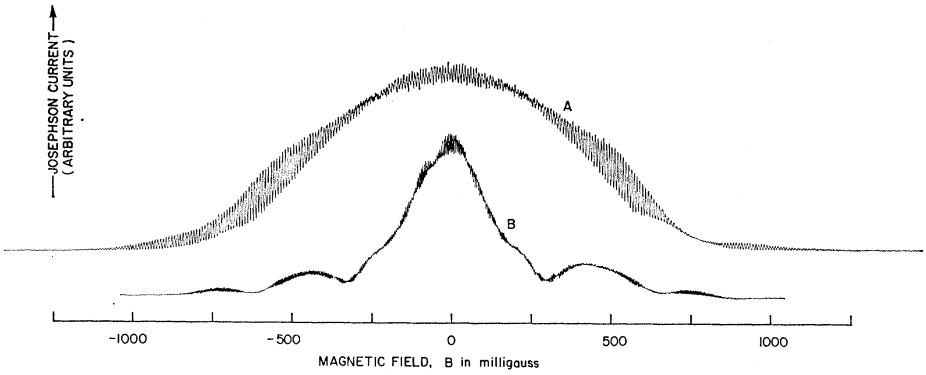

FIG. 8. Experimental trace of I_{max} versus applied field showing interference and diffraction effects. Interference periods are 8.7 and 4.8 mG for A and B, respectively. Maximum current in both cases was 1 mA.

using an ac technique with a 100-turn search coil. It was possible to identify defective coils by noting any deviation of behavior of one coil from the behavior of the others in the same batch, which gave identical results. Because of the internal consistency of these calibrations, it is believed that the coils used in the experiments were free from defects. The coils were built into a junction pair device by embedding them in the plastic insulation enclosed by the superconducting interferometer. At least 5 μ of plastic insulation separated the coil from the superconducting circuit. The second tin films were then deposited over the plastic in the usual manner.

EXPERIMENTAL RESULTS

Phase Modulation by a Magnetic Field

A series of 16 double-junction devices were measured for maximum Josephson current versus the applied magnetic field. Four of these are shown in Figs. 7 and 8. In all cases which could be checked, the smaller periodicity corresponded, within experimental limits, to a change in the enclosed flux of one quantum unit, $\Phi_0=h/2e$. The field periodicity of the samples ranged from 0.3 to 40 mG corresponding to areas from 7×10^{-4} to 5×10^{-6} cm^2. In most cases, as in the ones shown here, there were very definite diffraction effects causing a modulation of the interference pattern and in some instances the appearance of much smaller secondary maxima. In other cases, where junctions making up the pair showed signs of shorting, this attenuation of secondary diffraction maxima did not always occur and a more or less constant amplitude diffraction envelope was observed, contrary to ideal diffraction behavior. These large period modulations persist to the highest fields (20 G). Very likely an individual junction may have shorts localized in two or more points, the shorts behaving like Josephson junctions of very small area. Together these shorts show an interference pattern of their own with a field periodicity corresponding to areas comparable to the effective single junction area of $(2\lambda+t)w$. The tiny area of each short would have a very broad diffraction peak and would be unobservable in the field intensities obtainable here.

The particular pair represented by the curve in Fig. 7(a) was of especially low self-inductance relative to all the samples studied, as is indicated by the interference periodicity of 40 mG. For this reason, it is not surprising that of all the pairs studied, this one came closest to representing ideal behavior. In this case, $LI_0\simeq\frac{1}{6}\Phi_0$ which is just below the region where self-screening effects become important. This would explain why there is still a slight distortion of the shape of the interference peaks. It is very likely that both junctions had very nearly the same Josephson currents, although this could not be verified. The other three examples of the double junction behavior show various degrees of departure from the ideal interference patterns. Figure 7(b) is a junction for which $LI_0\simeq\Phi_0$ so that, although self-screening has become a factor, it has not severely distorted the pattern. The first diffraction side peaks are evident in this sample. An unbalance in the two junction Josephson currents could also be contributing to the reduced interference modulation. Figures 8(a) and 8(b) show two examples for cases where $LI_0>\Phi_0$, as might be expected from the small periods associated with the interference. In the both cases, the diffraction behavior is readily apparent, even though interference modulation is severely distorted and attenuated by the self-screening effects. The large over-all diffraction envelope of Fig. 8(b) corresponds to the junction width of 0.8 mm which was the larger of the two junctions. Both of these last curves show indications of unequal diffraction patterns for the two junctions as well as screening effects and for that reason are difficult to analyze in any detail, especially in the absence of detailed information of the behavior of the individual junctions.

Throughout the whole series of junction pairs studied, the period of the interference remained that change of field necessary to change the applied flux enclosed by the interferometer by one quantum unit. The biggest experimental uncertainty was in the determination of the enclosed area. This was due to the nonuniform thickness of the plastic film separator. For the smaller areas, the capacitance of this region was measured after isolation of the two films by removing the junction connections with a sharp needle. A dielectric constant of

TABLE I. Observed values of the interference period in applied flux obtained from magnetic-field and vector-potential modulation of the phases in units of 10^{-7} G cm². $h/2e=2.07\times10^{-7}$ G cm². Estimated errors in all cases are larger than the observed deviation from $h/2e$.

	$\Phi_0(B)$	$\Phi_0(A)$
	2.4	2.5	2.13±0.1
	2.6	2.4	2.15
	2.0	2.2	2.14
	2.2	1.9	2.05
Mean value	2.0		2.1

3.2 was assumed for the Formvar. For the larger areas, the area dimensions could be measured directly by focusing end-on with a 100× microscope equipped with a calibrated reticule. At best these methods gave 10 to 50% accuracy, which, as can be seen from the measured values of Φ_0 in Table I, is the approximate scatter of the observed flux values about the theoretical value. The periodicity associated with the interference was found to be almost totally independent of temperature, except for the smallest area junctions observed. For example, in the junction pair of Fig. 7(a) there was a change in the periodicity from 15.9 to 16.3 mG as the temperature was changed from 2.45 to 1.2°K. An estimate of the amount to be expected from the Gorter-Casimir theory of the temperature dependence of λ shows that this change is of the right size, assuming an effective area given by $(2\lambda+d)W$ where $d=0.41\,\mu$. In these experiments phase coherence in tin has been demonstrated up to distances of about 3 cm.

Phase Modulation by a Vector Potential

The observation of the interference due to the vector potential without the field penetrating the superconductor presented more of an experimental problem because of the necessity of using such a large enclosed area ($\approx5\times10^{-4}$ cm²) that self-screening effects made the measuring more difficult. Nevertheless, four successful devices were made which allowed the observation of periodicity when the flux through the solenoid was varied. As a best example, the curves shown in Fig. 9 exhibit the modulation due to the coil itself $\Phi(A)$ and on the same vertical scale that due to an applied field $\Phi(B)$. No diffraction effects are apparent with the coil modulation, as expected, even when many times the number of periods shown on this figure were covered. For the coil, the periodicity in flux as measured by the current exciting the coil was 16.9 μA per period, while the periodicity in field was 1.2 mG. From the coil calibration, this gives a value of the flux unit of $2.1\pm0.1\times10^{-7}$ G cm². From the area determination, which was much less accurate, the value is 1.9×10^{-7} G cm². The coil calibration is the most reliable one by far since direct electrical measurements could be made. For the four values of Φ_0 experimentally determined from the coil modulation, numbers within 5% of the theoretical flux unit were consistently obtained. Attempts were made to detect how much, if any, flux leakage occurred outside the coils. A small detector coil was placed close by and no observable signal was seen. This placed as an upper limit 0.01% of the field needed to produce the phase shift by means of a leakage field. To assure these effects were not due to an electric field (arising when the flux was changed), interference data were also taken at fixed values of flux, the flux being changed to a new value only while the interferometer was warmed to the normal state. In this technique the superconducting interferometer was used to measure a static flux in the absence of any electric or magnetic fields at the interferometer. Modulation of the maximum supercurrent was again observed under these circumstances presumably caused by the integrated static vector potential field directly. These results demonstrate, in a new way, the reality of the point made by Ehrenberg and Siday, and in addition give a quite accurate agreement with the theoretical flux unit. There is still room for improvement to measure the flux unit with greater accuracy.

A summary of the measured values of the flux unit from the two methods employed is presented in Table I. Only those values are included for the junction pairs whose area could be measured with reasonable accuracy. Also included are those value of Φ_0 taken from the coil modulation data. The agreement with theory in all cases is as close as experimental error allows.

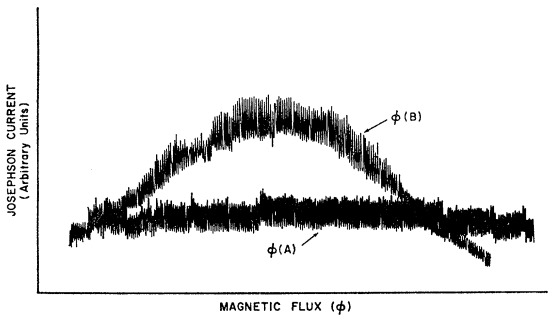

FIG. 9. Experimental trace of I_{max} versus applied flux for a junction pair showing modulation due to an applied field $\Phi(B)$ and vector potential above $\Phi(A)$. The field period is $\Delta B=1.2$ mG and the solenoid current period is 16.2 μA. The slight "beat" periodicity in both curves is a spurious effect due to a recorder defect.

Phase Modulation by Electron Motion

The third measurement is that of the phase modulation produced by motion of the superconducting electrons. The base film had a width of 4 mm, was 1100 Å thick, and was separated from its return strip by 5 μ of Formvar insulation. The width of both junctions was $\frac{1}{2}$ mm and their average separation was 8 mm. The modulation of the maximum Josephson currents through one such pair is shown in Fig. 10, where I_{max} is seen to be periodic with the drift current. There is also a general diffraction envelope as expected [see Eq. (17)] from the

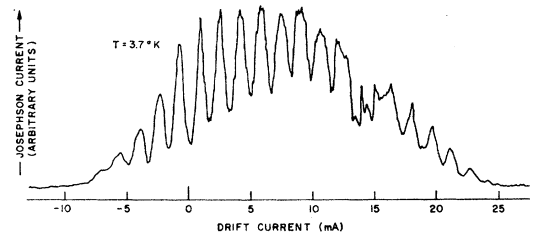

FIG. 10. Experimental trace of I_{max} versus the drift current showing interference and diffraction effects. The zero offset is due to a static applied field. Maximum current is 1.5 mA.

finite width of the junctions and a finite width resulting from an applied field. Secondary diffraction peaks could also be seen but are not shown here. In addition, there is the expected large dependence of the period on temperature. The ratio of the interference periods to the diffraction envelope remained constant over the entire temperature range studied and was equal to the ratio of the junction width to their separation (1:16) as expected. To check that this modulation was not due to a self-induced field, the magnetic field was measured 5 μ above the base film by another separate junction pair (not shown in Fig. 5) used as a magnetometer. The measured leakage field was less than 2×10^{-4} G for the maximum drift current employed. This would limit any possible leakage field effect to less than one-tenth of a single period. The period of the interference was studied as a function of temperature for two junction pairs, whose geometry and base film thickness were identical. The results from these two is shown in Fig. 11 where the periodicity of I_{max} is seen to increase rapidly as the temperature is lowered. This occurs because the decreasing penetration depth represents an increase in the density of superconducting electrons. The solid line represents a theoretical approximation of uniform current density at all temperatures and therefore represents only those effects directly attributable to changes in penetration depth. The dashed curve represents the curve calculated from Eq. (22) for the case where current distribution in the base film is taken into account. Both curves assumed that penetration depth at 0°K to be 720 Å which is a reasonable value for films. However, considering possible adjustments which could be made within the experimental uncertainty of the film thickness determination ($\pm$50 Å), this fit is considered a good one. We note that, in both the fitted

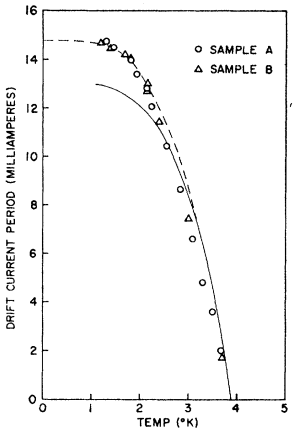

FIG. 11. Variation of observed drift-current period ΔI_D with temperature for two junction pairs of identical dimensions (w=0.5 mm and W=8 mm). The dashed curve is from Eq. (22) while the solid one is computed assuming uniform current density for all temperatures. The cross-section dimensions of the base film are 3 mm by 1100$\pm$50 Å.

curves, it was assumed that the charge and mass associated with the particles is that for pairs. The change in drift velocity Δv_D required to product a shift of one period is about 4.5 cm/sec, corresponding to a de Broglie wavelength $h(2mv_D)^{-1}$ of $\sim$1 cm.

CONCLUSIONS

We have presented here direct experimental evidence for the important and striking long-range coherence behavior in superconductors using a technique made possible by Josephson's discovery. This technique demonstrates that one can perform diffraction and interference experiments with the quantum waves associated with superconducting electrons and permits a particularly precise determination of the unit of flux $h/2e$. A new verification has been made of the idea of Ehrenberg and Siday and Aharonov and Bohm concerning the behavior of multiply connected quantum systems when acted on by a static vector potential alone, and provide an example where the paired nature of the superconducting particles plays an important role. The drift velocity experiment is a simple and direct measurement where motion of the pairs is observed and with which the detailed behavior of flux penetration in thin films can be measured.

ACKNOWLEDGMENTS

The authors wish to acknowledge the technical assistance of R. J. Blum in the film preparation and C. C. Mueller for fabrication of the solenoids.